



LAWRENCE
LIVERMORE
NATIONAL
LABORATORY

Scientific and Technological Advancements in Inertial Fusion Energy

D. E. Hinkel

March 15, 2013

Nuclear Fusion

Disclaimer

This document was prepared as an account of work sponsored by an agency of the United States government. Neither the United States government nor Lawrence Livermore National Security, LLC, nor any of their employees makes any warranty, expressed or implied, or assumes any legal liability or responsibility for the accuracy, completeness, or usefulness of any information, apparatus, product, or process disclosed, or represents that its use would not infringe privately owned rights. Reference herein to any specific commercial product, process, or service by trade name, trademark, manufacturer, or otherwise does not necessarily constitute or imply its endorsement, recommendation, or favoring by the United States government or Lawrence Livermore National Security, LLC. The views and opinions of authors expressed herein do not necessarily state or reflect those of the United States government or Lawrence Livermore National Security, LLC, and shall not be used for advertising or product endorsement purposes.

Scientific and Technological Advancements in Inertial Fusion Energy

D. E. Hinkel

Lawrence Livermore National Laboratory

LLNL-JRNL-627472

Scientific advancements in inertial fusion energy (IFE) were reported on at the IAEA Fusion Energy Conference, October 2012. Results presented transect the different ways to assemble the fuel, different scenarios for igniting the fuel, and progress in inertial fusion energy technologies. The achievements of the National Ignition Campaign within the USA, using the National Ignition Facility (NIF) to indirectly drive laser fusion, have found beneficial the achievements in other IFE arenas such as directly driven laser fusion and target fabrication. Moreover, the successes at NIF have pay-off to alternate scenarios such as fast ignition, shock ignition, and heavy ion fusion as well as to directly driven laser fusion. This synergy is summarized here, and future scientific studies are detailed.

INTRODUCTION

The prospect of inertial fusion energy (IFE) relies on scientific advancements in different arenas. In IFE, nuclear fusion reactions, initiated by heating and compressing a pellet that contains deuterium (D) and tritium (T), occur on a time scale shorter than (but comparable to) the disassembly time of the fuel. Ablation of the outer layers of the DT pellet, which is covered with ablator material, occurs, and the remaining target is accelerated inward. The central region of the target heats up, and is surrounded by a dense shell. If the central portion of the fuel is heated sufficiently, fusion reactions will occur, releasing energy. In a target heated and compressed to the point of thermonuclear ignition, energy can then heat surrounding fuel, causing it to fuse as well.

In this approach to IFE, known as central hot spot ignition, the capsule can be driven (ablated) by either x-radiation (indirect drive laser fusion, Fig. 1a), or by laser beams (direct drive laser fusion, Fig. 1b) [1]. Another approach to IFE is fast ignition (Fig. 1c), where the DT capsule is compressed to hundreds of grams/cc, and then a beam of laser-induced relativistic particles is transported to the imploded capsule, where sufficient energy is deposited in high-density plasma to create a local ignition hot spot [3-4]. A hybrid of this, known as shock ignition, is an approach where the fuel is compressed similarly as in fast ignition, and then high intensity laser beams striking the capsule further compresses the capsule to ignition conditions [5]. Finally, in heavy ion fusion [6-7], heavy ion beams convert to radiation, which drives the capsule implosion (c.f., Fig. 1d).

The National Ignition Facility (NIF) is a 192-laser beam facility that provides the opportunity for ignition physics research at full scale [8-9]. The indirect drive IFE approach has been under investigation at NIF since August, 2009. Achieving ignition requires: (i) sufficient laser energy coupling and x-ray conversion, to create; (ii) sufficient radiation drive on a thick enough (i.e., stable enough) shell, with; (iii) sufficient symmetry, such that (iv) fusion initiates in a central hot spot and a burn

front propagates outward. These processes are further detailed in Fig. 2. In Fig. 2a, laser beams are incident into a hohlraum, a cylinder composed of high-Z material, containing a DT capsule surrounded by a helium (He) gas fill. The laser beams enter the hohlraum through a laser entrance hole (LEH) in each cylinder endcap. The beams burn through a window covering the LEH and propagate to the wall, where conversion to x-radiation occurs. Laser energy coupling can be reduced by such laser-plasma interaction processes as backscatter, where the laser beams scatter off self-generated electron plasma or ion acoustic waves. Current energy coupling at NIF is $\sim 85\%$, which is good enough to investigate steps (ii)-(iv), but, ultimately, might be improved.

The x-radiation from the hohlraum walls fills the hohlraum, creating a radiation oven. The capsule is bathed in this radiation, the ablator heats up, and expands. X-ray drive diagnostics at NIF confirm that radiation temperatures of the order of ~ 300 eV (required for ignition) are being achieved. Finally, in step (iii), the ablated material expands outward, and, by conservation of momentum, the rest of the capsule accelerates inward. If there is more drive (or less drive) over the waist of the capsule than at the poles (LEH), the implosion will not be spherical, and will not compress as desired. This ratio can be changed by changing the power balance between the beams that propagate over the capsule (inner beams) vs the beams that hit the hohlraum wall closer to the LEH (outer beams). This power balance is achieved at NIF through the use of cross-beam energy transfer, where, energy is transferred from outer to inner beams at the LEH through forward Brillouin scatter, where laser light from an outer beam forward scatters into an inner beam. Finally, if sufficient compression and heating occurs, fusion initiates.

SYNERGY: COUPLING AND SYMMETRY

In terms of energy coupling and drive, E. I. Moses, in OV/1-4 [10], showed that symmetry at NIF is indeed achieved using cross-beam energy transfer [11](c.f. Fig. 3a). This is synergistic with direct drive coupling and 4ω drivers (KrF laser at wavelength 248 nm) in the following sense. With respect to direct drive, cross-beam energy transfer impacts laser coupling at the Omega laser. Therefore, a better understanding of cross-beam energy transfer at NIF, and how it impacts implosions, will provide pay-off to direct drive laser coupling. With respect to 4ω drivers, J. Sethian, IFE/1-4 [12], showed that a KrF laser has very uniform illumination, and because of the shorter wavelength, there should be better laser coupling. Further understanding of laser energy coupling of 4ω drivers will help guide future NIF laser improvements (c.f. Fig. 3b).

In IFE talk 1-3 [13], H. Shiraga discussed the status of fast ignition at ILE (c.f. Fig. 3c). The LFEX laser, used to produce fast electrons, has been improved by reducing the pre-pulse. The DD yield for fast ignition experiments at ILE is $\sim 3.5 \times 10^7$ neutrons [13]. Since, in fast ignition, the fuel is hydrodynamically assembled before hot electrons are generated and transported to the fuel core, and, since, hydrodynamic

assembly occurs at NIF, any improvements and/or insights at NIF with respect to hydrodynamic fuel assembly will impact future experiments at ILE.

In IFE poster IFE/P6-16 [14], Kwan showed progress on heavy ion fusion (c.f. Fig. 3d). The NDCX-II Induction Linac at LBNL is now complete. Here, heavy ion beams are converted to radiation, which drives the capsule implosion. Control of the radiation drive symmetry is important for both laser fusion and ion beam fusion.

SYNERGY: IMPLOSION AND BURN

There is also synergy between the indirect drive and direct drive IFE scenarios with respect to implosion and burn. In OV/1-4, E. I. Moses [10] showed the progress made toward achieving ignition. Adjustments to laser energy and power, along with shock timing have increased both the DT yield and the fuel areal density, ρr . Currently, the achieved fuel areal density is at 85% of what is required to enter the ignition regime. Moreover, the DT yield is within a factor of 4 of entering the self-heating regime. These accomplishments have transpired since the last IAEA FEC meeting, in 2010.

In IFE/1-2, R. L. McCrory [15] reported on progress in direct drive research at the Omega laser. NIF experiments in the polar direct drive configuration are planned, and to prepare for these, Omega symmetric direct-drive cryogenic target implosions are defining the NIF polar direct drive design space. Performance continues to improve, as measured by increases in both neutron yield and ion temperature. In Fig. 4, McCrory reports on the YOC (yield over clean) vs adiabat of the capsule. Here, YOC refers to the experimental yield to 1D simulated yield ratio. As the adiabat of the capsule increases, the YOC increases, attaining 40-50% of the 1D simulated values, and the ratio of experimental areal density to that predicted in 1D codes attains a value of 80-90%. This is most likely for a variety of reasons. A capsule on a higher adiabat converges less than a capsule on a low adiabat, which is less stressful on the symmetry requirements. In addition, with less convergence, mix of cold ablator into hot fuel will be reduced. Also, capsules on a higher adiabat are driven harder early in time, where they ablate more mass, providing more ablative stabilization. Such higher-adiabat implosions should be more robust to both high-mode and low-mode asymmetries. These important findings are being pursued for the indirect drive IFE scenario, as will be discussed later, another example of synergy among IFE scenarios.

The National Ignition Campaign (NIC) reports progress in terms of "ITFx", the experimental ignition threshold factor. ITFx depends on both yield and areal density (c.f. Figure 5a), or $ITFx \sim (Y/3.2e15)(dsr/0.07)^{2.3}$. Here, Y is the neutron yield, and dsr is the downscattered ratio, or the ratio of 10-12 MeV neutrons generated to 12-15 MeV neutrons. The dsr roughly scales as areal density/20.3 (from simulations). To date, $ITFx \sim 0.1$, where an increase of a factor of five is required to enter the self-heating regime.

The Laboratory for Laser Energetics at the University of Rochester reports [16] implosion progress in terms of $P\tau$, a generalized Lawson criterion, where $P\tau(\text{atm-s}) = 8[\langle\rho r\rangle\langle T\rangle]^{0.8}(YOC)^{0.4}$. Currently, Omega has achieved a $P\tau \sim 0.08 P\tau_{\text{ig}}$, or $\chi = (P\tau/P\tau_{\text{ig}}) \sim 0.08$. To scale up to ignition at the 1.8 MJ-NIF scale, Betti suggests that Omega-scale experiments must achieve a $P\tau \sim 0.16$. Folded into this suggestion are assumptions such as relatively smoother capsules due to an increase in scale size. Improving the current $\chi \sim 0.08$ to the goal of $\chi \sim 0.16$ also requires an implosion with a lower adiabat and higher velocity than is currently fielded. This challenging factor of two increase required for direct drive implosions is roughly equivalent to a factor of eight improvement in ITFx, since $ITFx \sim \chi^3$. With both indirect and direct drive implosions needing to improve in ITFx, there is potential for cross-fertilization.

FAST IGNITION, SHOCK IGNITION, HEAVY ION FUSION, AND X-RAY PINCHES

Progress on fast ignition at the Institute for Laser Engineering (ILE), at Osaka University, Japan, was reported on by H. Azechi, in OV/4-2 [13]. Upon completion and commissioning of the LFEX laser, experiments are achieving DD yields of $\sim 3.5 \times 10^7$ neutrons, and after pre-pulse suppression, $T_{\text{ion}} \sim 1$ keV has been achieved. The goal for FIREX experiments is $T_{\text{ion}} \sim 5$ keV. To realize these ion temperatures, the next step will be to impose an axial magnetic field that guides electrons to the capsule, and should further improve coupling of hot electrons to the fuel (c.f. Fig. 6b).

The U.S. fast ignition team has made significant progress on studying the details of fast ignition physics, using new platforms at the Omega laser facility (presented in poster IFE/P6-06 [18]). Omega experiments report the highest areal density achieved in a fast ignition, cone-in-shell implosion. The experimental results are qualitatively comparable to what is found in simulation (Fig. 7). This team has also performed fluorescent imaging of hot electron energy flow (Fig. 7), which shows energy flow into a sphere of radius $\sim 85 \mu\text{m}$. The challenge remains to achieve a reduction in fast electron beam divergence, reducing the hot electron energy deposition region to a sphere of radius $\sim 35\text{-}40 \mu\text{m}$.

It is interesting to note that both ion temperature and areal density are required to achieve ignition, with Japan reporting on the former, and the U.S. on the latter. These two approaches are complementary, and of benefit to both programs.

There are also alternate approaches to ignition that were presented at this conference (c.f. Fig. 8). In proton fast ignition (Fig. 8a), thin foil targets are illuminated with high laser intensity, and hot electrons exit the rear of the target. This establishes a sheath field, which ionizes and accelerates protons normal to the sheath. A key issue in using protons in fast ignition is whether the generated protons can be focused. Progress was reported on in IFE/P6-08 by McGuffey, and in IFE/P6-07, by Qiao [19-20]. Advances in the area include curving the foil from

whence protons are generated to focus the beam, and simulation studies of protons generated from curved foils.

Shock ignition can be thought of as an approach that is a hybrid of central hot spot ignition and fast ignition. In shock ignition, compression and hydrodynamic fuel assembly occurs as with fast ignition. Once the fuel is assembled, however, instead of generating relativistic particles, which transport their energy to the fuel, the same laser that compressed the fuel irradiates the target at high intensity, which drives a strong converging shock into the center of the fuel. There are still many physics issues to be addressed before this is a viable IFE scenario, but work is ongoing in this area (S. Jacquemot, IFE/PD) [21].

Another alternative IFE scenario is the heavy ion “X” target, a hybrid approach of fast ignition and heavy ion fusion. As shown in Fig. 8b, the heavy ion X target is a simple axisymmetric target with deuterium-tritium (DT) filling a metal case with a cross section in the shape of an X. Also shown in Fig. 8b is the location of the three annuli of heavy-ion beams used for compression as well as the solid central beams overlapping on axis used for ignition. The cylindrical X-target is a novel heavy ion beam driven high-gain IFE target. The axial beam illumination is transformed to radial implosion, followed by an ultra-short pulse fast ignition at the cone tip. Explanation and progress of this concept was reported on in IFE/P6-16 by Kwan [14].

In IFE/P6-17, Gourdain [22] reported on magnetic field compression studies. Gourdain discusses gas puff z-pinchs and thin liners, and the stabilizing effects of axial magnetic fields. Shown in Fig. 8d is an XUV image of such an x-ray pinch. This work is tied to the MagLIF IFE concept, where fusion conditions are achieved in a hydrogen plasma by imploding a cylindrical liner onto the fusion fuel [22]. This concept relies on using a laser to preheat the plasma, but these aspects of this IFE scenario were not discussed at this meeting.

IFE TECHNOLOGIES

To this point, we have discussed the different ways in which inertial confinement could be achieved, and the advances reported. However, an inertial fusion energy power plant relies on a target factory, a target injection system, a high average power laser, reactor chamber protection, and a power conversion system. Advances in both drivers and these technology areas are crucial to IFE.

With respect to drivers (c.f. Fig. 9a), Mori, IFE/P6-13 [23], reported on advances with high rep-rate lasers. A DPSSL-pumped laser, HAMA, a 10-J class DPSSL, is now used in ICF experiments and succeeded in DD neutron generation. Based on HAMA, design and development of an integrated repetitive ICF experiment machine can now go forward, which would include other indispensable IFE technologies such as target injection and tracking. In IFE 1-4, Sethian [12] reported on KrF lasers directly driving fusion targets. Analyses indicate 300 - 700 J/pulse, 2.5 - 5 Hz, 10 hour continuous run, and predictions of > 7% efficiency. And, of course, there is the

ability to look at 2ω (527 nm “green” light) driven implosions on NIF, and compare to the current 3ω (351 nm “blue” light) driven implosions.

With respect to heavy ion beam drivers (c.f. Fig. 9b), Kwan (IFE/P6-16) [14] reported that a new ion accelerator user facility, NDCX-II, was completed at LBNL in 2012. It is an induction linac designed to accelerate and compress an MeV Li^+ ion beam bunch to ~ 1 ns for rapid volumetric heating of a thin foil target. This facility provides excellent opportunities for studying warm, dense matter as well as the physics of ion beam compression with plasma neutralization for HIF drivers. Ultimately, the vision is to drive an IFE target with 20 GeV Rubidium beams, which provides a simulated yield of 1.5 GJ [24].

Target fabrication, injection and tracking are also being studied. Azechi, OV/4-2 [17], reported that at ILE/OSAKA, mass production of targets, target injection, and target tracking are under scientific investigation (Fig. 9c). He reports that tracking to 1 μm precision has been demonstrated.

Reactor chamber protection is also important to IFE. Analyses on how to mitigate chamber damage due to ions, neutrons and cyclic stresses include use of liquid walls, comprised of “materials on demand”, designed at nanoscale with sufficient mechanical strength and radiation resistance, as well as using improved rapid change-out techniques.

As scientific advances are made among the different scenarios by which inertial confinement can be achieved, these technologies will become of the utmost importance. It is thus important to continue to make technological advances in these arenas, in preparation for ignition in a laboratory setting.

NATIONAL IGNITION CAMPAIGN RESULTS AND FUTURE PROSPECTS

There have been ignition science advances made within the last few years by the National Ignition Campaign [25-29]. These advances were enabled by the achievable laser power and energy of the National Ignition Facility, as well as its precision. In July 2012, this facility surpassed its milestone of delivering 1.8 MJ of laser energy at 3ω , and 500 TW of laser power on target. E. I. Moses [10] reported on this accomplishment, 1.855 MJ and 522 TW, in OV/1-4 (c.f. Fig. 10a). The precision of NIF is the basis for exquisite tuning and reproducibility. Shown in Fig. 10b are target chamber center (TCC) power requests for a particular shot on May 21, 2011 (N110521). Shown in black is the request, and overlying the black curves is the power delivered to the inner cones (red), the outer cones (green), and the total power delivered (blue). Without such capabilities, the ignition campaign would not be where it is today.

To further the scientific understanding, there are several areas of study currently being pursued on the National Ignition Facility. First, there is an effort underway to better understand and to improve laser coupling to the indirect drive target

(hohlraum). One of the struggles of laser energy coupling to the target has been poor propagation of the inner beams, the laser beams with long path lengths to the wall, over the capsule [30-31]. Improvement of inner beam propagation reduces the amount of energy transfer from the outer beams required to achieve a round implosion.

To test this, a rugby hohlraum [32] is being fielded at NIF in FY13. The rugby hohlraum (c.f. Fig. 11a) provides more headroom over the capsule for the same surface area of the hohlraum wall. When mass is ablated from the capsule and the wall, there is not as great of a build-up of density over the capsule, and thus, the beams should propagate better. In current designs of rugby hohlraums, no cross-beam energy transfer is required to get a round implosion. The targets are currently being fabricated, and results will be reported on later in the year.

There is also an effort underway to reduce stimulated Raman scattering (SRS) in ignition hohlraums, where incident laser light backscatters off self-generated electron plasma waves [Ref.32, and references therein]. In such hohlraums, SRS is reduced (according to linear theory, because of stronger Landau damping) as the electron temperature increases. One way to increase the electron temperature is to propagate the beams through a gas fill with a higher Z, resulting in higher levels of inverse bremsstrahlung [33].

To test this idea, room temperature targets are being fielded at NIF, with a C_5H_{12} gas fill (such fills cannot be fielded cryogenically, as they freeze out). If a higher-Z fill proves to be advantageous at room temperature, then cryogenic analogies, such as foam doped with high-Z composites will be investigated. If such targets do result in lower backscatter, inner beam propagation to the wall might also improve.

Not only is SRS a direct energy loss (through backscatter), but this process also produces hot electrons (c.f. Fig. 11b). Hard x-ray images of the capsule and environs [34] show no evidence of hot electrons coupling to the capsule at levels sufficient enough to cause serious preheat, but it is nonetheless important to test this further, by either a reduction in SRS (as discussed above), or by changing the flavor of backscatter to stimulated Brillouin scattering (SBS), where incident laser light backscatters off self-generated ion acoustic waves [Ref. 32, and references therein]. NIF hopes to investigate an “SBS-only” target in the near future.

Once the rugby hohlraum is fielded, and the energy coupling is determined, as well as whether the energy loss is primarily SRS or SBS, decisions will be made about how to (i) further reduce backscatter (by increasing the electron temperature), and (ii) if necessary, change the fill composition to produce SBS instead of SRS.

Finally, there is the prospect of new diagnostics to further research energy coupling. It is very desirable to consider plasma characterization via 4ω Thomson scatter [35] (c.f. Fig. 11c). To date, the only diagnostic of plasma conditions within the hohlraum is the SRS spectrum, which provides information through the scattered wavelength

about the density and temperature of the region in which SRS occurs. Plasma characterization would serve to more tightly constrain hohlraum modeling as well as the reduced model physics contained in the radiation-hydrodynamics simulations.

In IFE/P6-10, C. K. Li [36] discussed using proton deflectometry [37] (c.f. Fig. 11c) to characterize electric fields within the capsule and perhaps within the hohlraum. Providing such information helps to further constrain modeling of such targets.

Lastly, current ignition targets depend on cross-beam energy transfer [11] to achieve symmetry. Stand-alone codes calculate the effect of cross-beam transfer on the laser spots (c.f. Fig. 11c), but there is no validation of these simulations. To further characterize cross-beam energy transfer, time has been allotted on the NIF laser to shoot a target where cross-beam energy transfer occurs, and then is x-ray imaged on a witness plate. These experiments will, again, further constrain parameter space, as well as provide more detailed information about the non-uniformity of laser beams after transfer.

NIF also plans to further investigate low mode asymmetry in the assembled fuel. Neutron data (c.f. Fig. 12a, Frenje, IFE/1-1 [38]) suggest such low mode asymmetry exists. Images of the neutron source and high-density shell were discussed by J. Frenje, IFE/1-1. Such asymmetry might be caused by the hohlraum drive, or by low modes in the ablator and/or DT ice layer.

In OV/1-4, E. I. Moses [10] presented simulation results of B. K. Spears, where low mode asymmetry (modes = 1,2,3) is introduced at peak power (c.f. Fig. 12b). Results from these simulations begin to match observables, such as the yield, pr, and ion temperature. Moreover, the similarities are striking, upon comparison of Fig. 12b to Fig. 12a. In OV/1-4, E. I. Moses [10] also discussed how present x-ray images capture hot spot self-emission only, which appear centered, as shown in Fig. 12c. These x-ray images do not provide any information about cold fuel shape. To investigate the shape of the cold fuel, backlit experiments are underway. Current findings indicate a mode 4 asymmetry, and future experiments will investigate (i) the cause of this asymmetry, and (ii) control of said asymmetry.

Finally, scientific understanding and mitigation of mix at NIF is being explored through a variety of different platforms. Data from the National Ignition Campaign shows a sharp performance boundary due to mix. High mode asymmetry, such as shown in Fig. 13a, was presented in OV/1-4 by E. I. Moses [10]. Such asymmetry is caused by surface roughness on the ablator surfaces as well as on the ice surfaces, as well as by minute dust particles on the outer ablator surface. Mitigation of high mode asymmetry occurs as target fabrication techniques improve and provide smoother ice layers and ablators; and by reducing dust on the outside of the capsule, which is introduced as the target is assembled. Another mitigation strategy is to field a higher adiabat implosion, as suggested by R. L. McCrory, in IFE/1-2 [15]. A higher adiabat implosion undergoes less convergence, and thus perturbations on

the surface grow exhibit lower growth factors for most of the Legendre modes. Also contributing to lower growth factors is the enhanced ablative stabilization that occurs for a higher adiabat implosion. When cryogenic implosions at a higher adiabat are fielded at the Omega laser, a higher YOC (experimental yield to clean, 1D simulated yield) is achieved, demonstrating these effects.

Figure 13b exhibits a plot of the maximum simulated growth factor (amplitude of the positive lobe) as a function of peak velocity at the fuel-ablator interface. The purple squares which lie along an isoadiabat ~ 1.6 depict the maximum growth factor for ignition designs, derived from simulations. The green circles illustrate the growth factor derived from post-shot simulations of NIF layered shots, also lying along an isoadiabat ~ 1.6 . A deliberate mistiming was introduced late in time to simulations, and the growth factors for simulations with these late mistimings lie along an isoadiabat ~ 2 , shown by the blue diamonds. Further, when a mistiming is introduced to simulations earlier in time, so that the 3rd shock overtakes the 2nd before entering the capsule DT gas, growth factors are even lower, as delineated by the red circles, lying along an isoadiabat ~ 3 . With capsule implosions on an adiabat ~ 2.3 , but with shocks timed to merge at the appropriate depths, growth factors are even lower, as depicted by the magenta and black happy faces. Placing the capsule on a high adiabat early in time suggests less mix, though at the cost of reducing yield.

The same is true for maximum simulated growth factors vs peak velocity at the ablation front, i.e., the HiFoot design maximum is lower than those of post-shot simulations (at a given velocity). However, while the minimum of the simulated growth factor (amplitude of the negative lobe) at the fuel-ablator interface is typically lower for the HiFoot design, that is not true of the minimum growth factor at the ablation front. If the minimum lobe of the ablation front growth factor is the dominant feature, then the HiFoot performance may not improve over that of 2012 NIC shots.

Currently this hypothesis is being tested at NIF. Figure 13c shows Tr vs time for the “HiFoot” capsule. The radiation drive has a foot temperature of ~ 85 eV, as compared to 60 eV for the nominal ignition capsule. A HiFoot campaign is currently underway at NIF.

SUMMARY

There has been significant progress in sculpting the building blocks for IFE (c.f. Figure 14). The NIF of today reports tremendous achievements: great laser performance, achieving 85% of the areal density required for ignition, but the yield and hot spot pressure are low. The focus of NIF over the next few years will be on addressing the causes of low yield and hot spot pressure.

For Alternate Scenarios, direct drive experiments, such as those at the Omega laser, report an improvement in performance. Further improvement in performance (higher implosion velocity, lower adiabat) is required for ignition (Betti, OV/5-3

[16]). Thus, both indirect and direct drive scenarios face the challenge of improving implosion performance, and both approaches will benefit from cross-fertilization.

Fast Ignition reports from Japan demonstrated the performance of LFEX with an improved pre-pulse, achieving a Tion ~ 1 keV with a DD yield of $\sim 3.5 \times 10^7$ neutrons. The US team reported on an improvement in areal density achieved. Both simulations and experimental diagnostics show fast electron energy deposition into a sphere ~ 85 μm . The ILE team plans to investigate the impact of axial magnetic fields on fast electron divergence. Shock Ignition analyses are underway, and should be reported on at the next FEC.

Improvements in IFE technologies were also reported. Research is ongoing in the areas of drivers, targets, target injection systems and reaction chambers.

The NIF of Tomorrow, which has become the NIF of Today, is exploring improvements and scientific understanding to further the ignition effort using indirect drive. Explorations on how to improve laser energy coupling to the target are underway, as are diagnoses of low mode asymmetries. An extensive mix campaign is a part of the high energy density physics being studied at NIF, and targets that might show a higher robustness to mix will be fielded on NIF in FY13.

All of the above have interrelated synergies, and when successes occur in one area, that will trigger success in other areas. Progress across all of these scientific and technological endeavors brings us closer to our ultimate goal, an optimized IFE reactor.

ACKNOWLEDGMENTS

This work was performed under the auspices of the U.S. Department of Energy by Lawrence Livermore National Laboratory under Contract DE-AC52-07NA27344. The author thanks the Programme Committee for the invitation to prepare this IFE summary. The author also thanks the other IAEA FEC authors who provided information for this IFE summary. The author acknowledges valuable input from J. D. Lindl, and M. D. Rosen.

REFERENCES

- [1] J. H. Nuckolls, L. Wood, A. Theissen, and G. B. Zimmerman, *Nature* **239**, 139 (1972).
- [2] J. D. Lindl, *Inertial Confinement Fusion* (Springer-Verlag, New York, 1998), pp. 1-15.
- [3] Max Tabak, James Hammer, Michael E. Glinsky, William L. Kruer, Scott C. Wilks, John Woodworth, E. Michael Campbell, Michael D. Perry, and Rodney J. Mason, *Phys. Plasmas* **1**, 1626 (1994).
- [4] D. J. Strozzi, M. Tabak, D. J. Larson, L. Divol, A. J. Kemp, C. Bellei, M. M. Marinak, and M. H. Key, *Phys. Plasmas* **19**, 072711 (2012).
- [5] R. Betti, C. D. Zhou, K. S. Anderson, L. J. Perkins, W. Theobald, and A. A. Solodov, *Phys. Rev. Lett.* **98**, 155001 (2007).
- [6] Max Tabak and Debra Callahan-Miller, *Phys. Plasmas* **5**, 1895 (1998).
- [7] Debra A. Callahan-Miller and Max Tabak, *Phys. Plasmas* **7**, 2083 (2000).
- [8] J. A. Paisner, E. M. Campbell, and W. J. Hogan, *Fusion Technol.* **26**, 755 (1994).
- [9] E. Moses, R. Boyd, B. Remington, C. Keane, and R. Al-Ayat, *Phys. Plasmas* **16**, 041006 (2009).
- [10] E. I. Moses, IAEA FEC 2012, OV/1-4, "The National Ignition Campaign (NIC): Status and Progress", submitted to Nuclear Fusion (January 2013).
- [11] P. Michel, S. H. Glenzer, L. Divol, D. K. Bradley, D. Callahan, S. Dixit, S. Glenn, D. Hinkel, R. K. Kirkwood, J. L. Kline, W. L. Kruer, G. A. Kyrala, S. Le Pape, N. B. Meezan, R. Town, K. Widmann, E. A. Williams, B. J. MacGowan, J. Lindl, and L. J. Suter, *Phys. Plasmas* **17**, 056305 (2010).
- [12] J. Sethian in Fusion Energy 2012 (Proc. 24th Int. Conf. San Diego, 2012), IFE/1-4, <http://www-naweb.iaea.org/napc/physics/FEC/FEC2012/index.htm>.
- [13] H. Shiraga, in Fusion Energy 2012 (Proc. 24th Int. Conf. San Diego, 2012), IFE/1-3, <http://www-naweb.iaea.org/napc/physics/FEC/FEC2012/index.htm>.
- [14] J. Kwan in Fusion Energy 2012 (Proc. 24th Int. Conf. San Diego, 2012), IFE/P6-16, <http://www-naweb.iaea.org/napc/physics/FEC/FEC2012/index.htm>.

- [15] R. L. McCrory, IAEA FEC 2012, IFE/1-2, "Progress toward Polar-Drive Ignition for the NIF", San Diego, CA, submitted to Nuclear Fusion (January 2013).
- [16] R. Betti, IAEA FEC 2012, OV/5-3, "Theory of Ignition and Hydro-equivalency for Inertial Confinement Fusion", submitted to Nuclear Fusion (January 2013).
- [17] H. Azechi, IAEA FEC 2012, OV/4-2, "Present Status of Fast Ignition Realization Experiment and Inertial Fusion Energy Development", San Diego, CA, submitted to Nuclear Fusion (April 2013).
- [18] M. S. Wei in Fusion Energy 2012 (Proc. 24th Int. Conf. San Diego, 2012), IFE/P6-06, <http://www-naweb.iaea.org/napc/physics/FEC/FEC2012/index.htm>.
- [19] C. McGuffey in Fusion Energy 2012 (Proc. 24th Int. Conf. San Diego, 2012), IFE/P6-08, <http://www-naweb.iaea.org/napc/physics/FEC/FEC2012/index.htm>.
- [20] B. Qiao in Fusion Energy 2012 (Proc. 24th Int. Conf. San Diego, 2012), IFE/P6-07, <http://www-naweb.iaea.org/napc/physics/FEC/FEC2012/index.htm>.
- [21] S. Jacquemot in Fusion Energy 2012 (Proc. 24th Int. Conf. San Diego, 2012), IFE/PD, <http://www-naweb.iaea.org/napc/physics/FEC/FEC2012/index.htm>.
- [22] P-A Gourdain, IAEA FEC 2012, IFE/P6-17, and references therein, "Axial Magnetic Field Compression Studies Using Gas Puff Z-pinches and Thin Liners on COBRA", submitted to Nuclear Fusion (January 2013).
- [23] Y. Mori, IAEA FEC 2012, IFE/P6-13, "Green DPSSL-pumped Laser System HAMA for High-repetitive Counter Irradiation Fast Heating Fusion Demonstration", submitted to Nuclear Fusion (January 2013).
- [24] E. Henestroza, B. G. Logan, and L. J. Perkins, *Phys. Plasmas* **18**, 032702 (2011).
- [25] J. D. Lindl and E. I. Moses, *Phys. Plasmas* **18**, 051001 (2011);
- [26] O. L. Landen, J. Edwards, S. W. Haan *et al.*, *Phys. Plasmas* **18**, 051002 (2011);
- [27] M. J. Edwards, J. D. Lindl, B. K. Spears *et al.*, *Phys. Plasmas* **18**, 051003 (2011);
- [28] N. B. Meezan, A. J. MacKinnon, D. G. Hicks, E. L. Dewald, R. Tommasini, S. Le Pape, T. Döppner, T. Ma, D. R. Farley, D. H. Kalantar, P. Di Nicola, D. A. Callahan, H. F. Robey, C. A. Thomas, S. T. Prisbrey, *et al.*, *Phys. Plasmas* **20**, 056311 (2013).
- [29] J. L. Kline, D. A. Callahan, S. H. Glenzer, N. B. Meezan, J. D. Moody, D. E. Hinkel, O.

S. Jones, A. J. MacKinnon, R. Bennedetti, R. L. Berger, D. Bradley, E. L. Dewald, I. Bass, C. Bennett, M. Bowers, *et al.*, *Phys. Plasmas* **20**, 056314 (2013).

[30] D. E. Hinkel *et al.*, *Phys. Plasmas* **18**, 056312 (2011);

[31] Rosen, M.D., Scott, H.A., Hinkel, D.E., Williams, E.A., Callahan, D.A., Town, R.P.J., Divol, L., Michel, P.A., Kruer, W.L., Suter, L.J., London, R.A., Harte, J.A., and Zimmerman, G.B., *HEDP* **7**, 180 (2011).

[32] Peter Amendt, C. Cerjan, D. E. Hinkel, J. L. Milovich, H.-S. Park, and H. F. Robey, *Phys. Plasmas* **15**, 012702 (2008).

[33] S. Rand, *Phys. Rev.* **136**, B231 (1964); B. A. Tozer, *Phys. Rev.* **137**, A1665 (1965).

[34] T. Döppner *et al.*, *Rev. Sci. Instrum.* **83**, 10E508 (2012).

[35] D. H. Froula, J. S. Ross, L. Divol, and S. H. Glenzer, *Rev. Sci. Instrum.* **77**, 10E522 (2006).

[36] C. Li, IAEA FEC 2012, IFE/P6-10, “Proton Imaging of Hohlraum Plasma Stagnation in Inertial Confinement Fusion Experiments”, submitted to Nuclear Fusion (December 2012).

[37] C. K. Li *et al.*, *Rev. Sci. Instrum.* **77**, 10E725 (2006).

[38] J. Frenje, IAEA FEC 2012, IFE/1-1, “Diagnosing Implosion Performance at the National Ignition Facility by Means of Advanced Neutron-Spectrometry and Neutron-Imaging Techniques”, submitted to Nuclear Fusion (December 2012).

FIGURE CAPTIONS

Fig. 1. The prospect of inertial fusion energy derives from advancement in different scientific arenas. **(a)** Central hot spot ignition using indirectly driven laser fusion, where laser beams generate x-radiation, which drives a capsule filled with deuterium (D) and tritium (T) to fusion conditions. **(b)** Central hot spot ignition using directly driven laser fusion, where laser beams hit the capsule and compress it to fusion conditions. **(c)** Fast ignition, where fuel is hydrodynamically assembled, after which relativistic particles transported to the central hot spot deposit their energy and initiate fusion; and, shock ignition, where fuel is hydrodynamically assembled, after which lasers at high intensity strike the capsule and shock it to conditions where fusion is initiated. **(d)** Heavy ion fusion, where ion beams are converted to radiation, which then drives the implosion.

Fig. 2. The processes entailed in indirectly driven laser fusion. **(a)** Coupling: laser energy enters the hohlraum target, which encloses a pellet of DT encased in ablator material, strikes the hohlraum walls, as is converted to x-radiation. **(b)** Drive: The x-radiation fills the hohlraum, creating a radiation oven that bathes the capsule, and the ablator heats up. **(c)** Symmetry: the ablated shell expands outward, and the remainder of the capsule is compressed inward (conservation of momentum). If the capsule does not remain nearly spherical while being compressed, it will not achieve conditions required for fusion initiation. **(d)** Fusion: initiates in a central hot spot where the ion temperature is high, and a burn front propagates outward.

Fig. 3. Synergy between different IFE scenarios drives progress in ignition science with respect to energy coupling and drive. **(a)** At NIF, symmetry is achieved using cross-beam energy transfer. **(b)** At Omega, cross-beam energy transfer is deleterious to the implosion, as incident laser beams can give up energy to the sides of other beams that miss the capsule. Understanding of cross-beam energy transfer facilitates both indirectly and directly driven implosions. This work will also enable implosions driven with 4ω lasers, and the success of 4ω implosions has impact on the NIF of the future. **(c)** NIF and Omega progress at hydrodynamic assembly of fuel paves the way for fast ignition, where the fuel is assembled prior to the transport of relativistic particles to the core. **(d)** Heavy ion fusion converts ion beam energy to radiation in radiation converters. Symmetry of radiation as seen by the capsule is important in both laser and ion beam fusion.

Fig. 4. Direct drive ICF research has made significant progress since the 2010 IAEA meeting. Performance of Omega cryogenic implosions improves at higher adiabat, a result that is currently being test at NIF. Experimental areal density achieved at higher adiabat is approximately 90% that of a clean, 1D simulation.

Fig. 5. Synergy between different IFE scenarios drives progress in ignition science with respect to implosion and burn. **(a)** The National Ignition Campaign has achieved 85% of the areal density required for fusion initiation, and is within a factor of a few of the self-heating regime. Progress is reported in terms of an

experimental ignition threshold factor (ITFX). Adjustments to the laser pulse energy and duration, as well as shock timing, have contributed to increases in ITFX. **(b)** Hydro-equivalent ignition on Omega is reported in terms of $P\tau$, where a value of $0.16 \cdot P\tau_{ig}$ is necessary. Both Omega and NIF implosions require a factor of two increase to meet this criterion.

Fig. 6. Fast ignition at ILE, University of Osaka, Japan: yield and Tion have exceeded previous records, with a path for further improvement. **(a)** Neutron yield and Tion is commensurate with $\sim 20\%$ coupling efficiency, with Tion ~ 1 keV. **(b)** Magnetic field guiding of hot electrons to the core should further improve coupling, with the prospect of achieving Tion ~ 5 keV.

Fig. 7. The U.S. fast ignition team has made significant scientific progress. The areal density achieved at the Omega EP laser has measured the highest areal density ($\rho r \sim 0.3$ g/cm²) of a fast ignition target, and the result is in qualitative agreement with simulation. Experimental Cu-K α images elucidate fast electron flow in these targets.

Fig. 8. Reports on alternate scenarios for achieving inertial confinement fusion.

- (a)** Proton fast ignition, where relativistic protons deposit energy in the hydrodynamically assembled fuel. Proton beam focusing enhances coupling.
- (b)** Shock ignition laser power vs time. The portion of the pulse colored “gold” hydrodynamically assembles the fuel. The portion of the pulse colored “red” shock compresses the capsule to fusion conditions.
- (c)** Heavy ion X-target uses heavy ion beams to assemble the fuel, and a fast ignitor beam to initiate fusion.
- (d)** X-ray Pinch: XUV image of axial magnetic field compression studies.

Fig. 9. Advances in drivers and technology are crucial for IFE. **(a)** A DPSSL-pumped, 10-J class laser, HAMA, is now used in ICF experiments. Analyses of KrF lasers directly driving fusion targets indicate 300 - 700 J/pulse, 2.5 - 5 Hz, 10 hour continuous run, and predictions of $> 7\%$ efficiency. Implosions driven with 2ω laser light is a future option for NIF. **(b)** A new ion accelerator user facility, NDCX-II, was completed at LBNL in 2012. It is an induction linac designed to accelerate and compress an MeV Li⁺ ion beam bunch to ~ 1 ns for rapid volumetric heating of a thin foil target. **(c)** Target fabrication, injection and tracking: mass production of targets, target injection, and target tracking are under scientific investigation. Tracking to 1 μ m precision has been demonstrated. **(d)** Analyses on how to mitigate chamber damage due to ions, neutrons and cyclic stresses include use of liquid walls, comprised of “materials on demand”, designed at nanoscale with sufficient mechanical strength and radiation resistance, as well as using improved rapid change-out techniques.

Fig. 10. NIF, with its power and energy capabilities, is truly a premier facility for future ignition physics studies. **(a)** NIF is capable of delivering in excess of 1.8 MJ of

3 ω energy and 500 TW of power. **(b)** The precision of NIF is the basis for exquisite tuning and reproducibility.

Fig. 11. NIF plans to field a variety of targets to explore laser energy coupling improvements. **(a)** Improve inner beam propagation, which reduces need for cross-beam energy transfer. A change in hohlraum geometry tests the impact of hohlraum shape on inner beam propagation. The first attempt at this will be in a rugby hohlraum. To increase electron temperature, which should enhance beam propagation to the wall, a change in hohlraum fill is being investigated. **(b)** Reduction in SRS and thus hot electrons tests SBS-only targets. An increase in electron temperature and a change in hohlraum fill is the path forward. **(c)** The prospect of new diagnostics and new experiments better characterizes both plasma and laser beam conditions. Thomson scatter and proton deflectometry characterizes plasma conditions. Cross-beam energy transfer experiments help characterize laser beam spots after transfer.

Fig. 12. NIF is fielding new backlighter diagnostics to further diagnose low mode asymmetries. **(a)** Neutron imaging suggests an offset in the hot spot with respect to the high density shell, **(b)** an effect which is seen in simulations where a small amplitude, low-mode asymmetry is introduced during peak power. **(c)** Present images capture only self-images of the hot spot emission. Backlit experiments to measure cold fuel shape have begun.

Fig. 13. NIF will field lower convergence, higher stability implosions to scientifically investigate mix mitigation. **(a)** Data shows a sharp performance boundary with respect to mix. Mix is caused by surface roughness (on all surfaces) and by minute dust capsules on the outer ablator surface. **(b)** Simulations of higher adiabat implosions show a greater robustness to mix, as evidenced by lower growth factors. **(c)** The NIF high-adiabat design, at $\alpha=2.3$, results in an ~ 85 eV temperature in the radiation foot, as compared to 60 eV in a nominal implosion. Omega has demonstrated more 1D-like results for higher adiabat implosions, and NIF is pursuing this with the indirect drive approach.

Fig. 14. There has been significant progress in sculpting the building blocks for IFE reported at this IAEA FEC. Successes in one arena triggers success in other arenas. Ultimately, an optimized IFE reactor will emerge from these scientific endeavors.

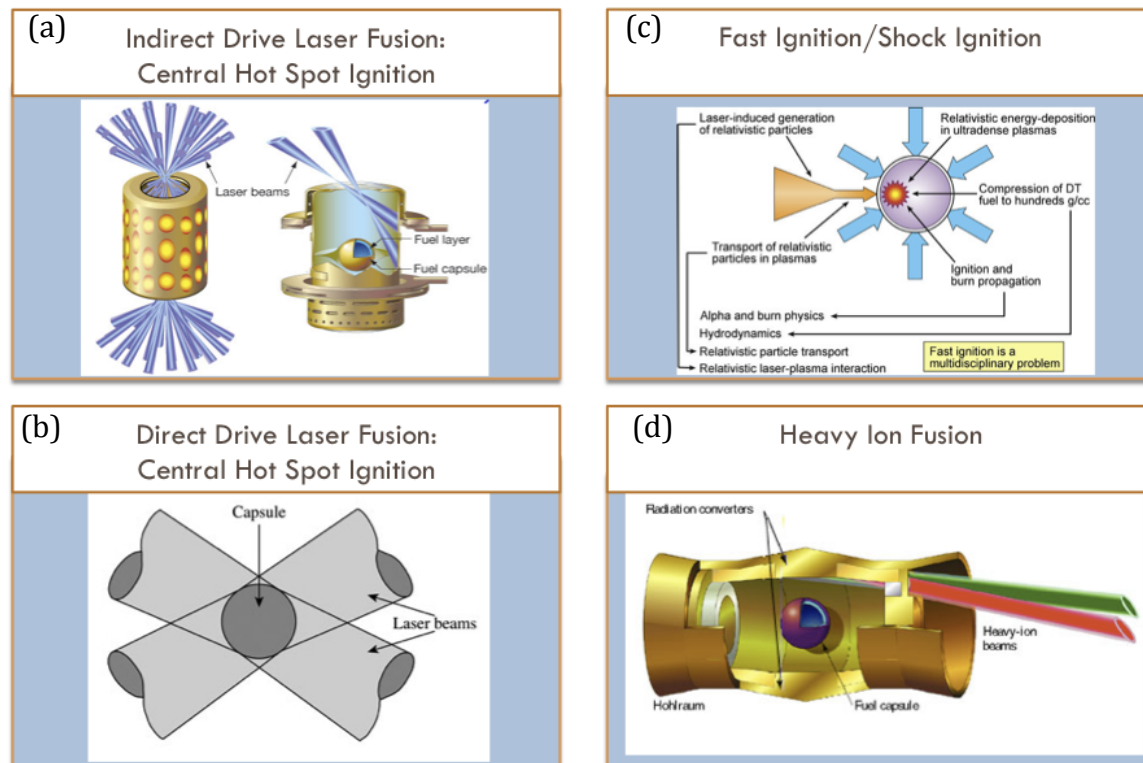


Fig. 1

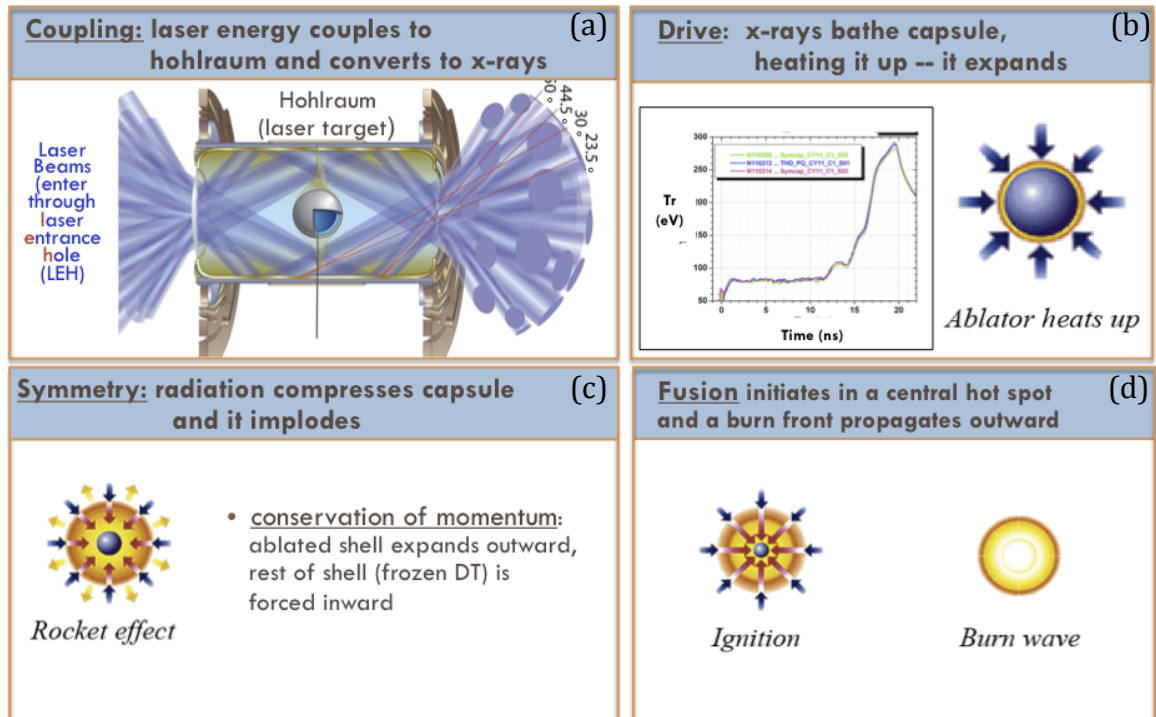


Fig. 2

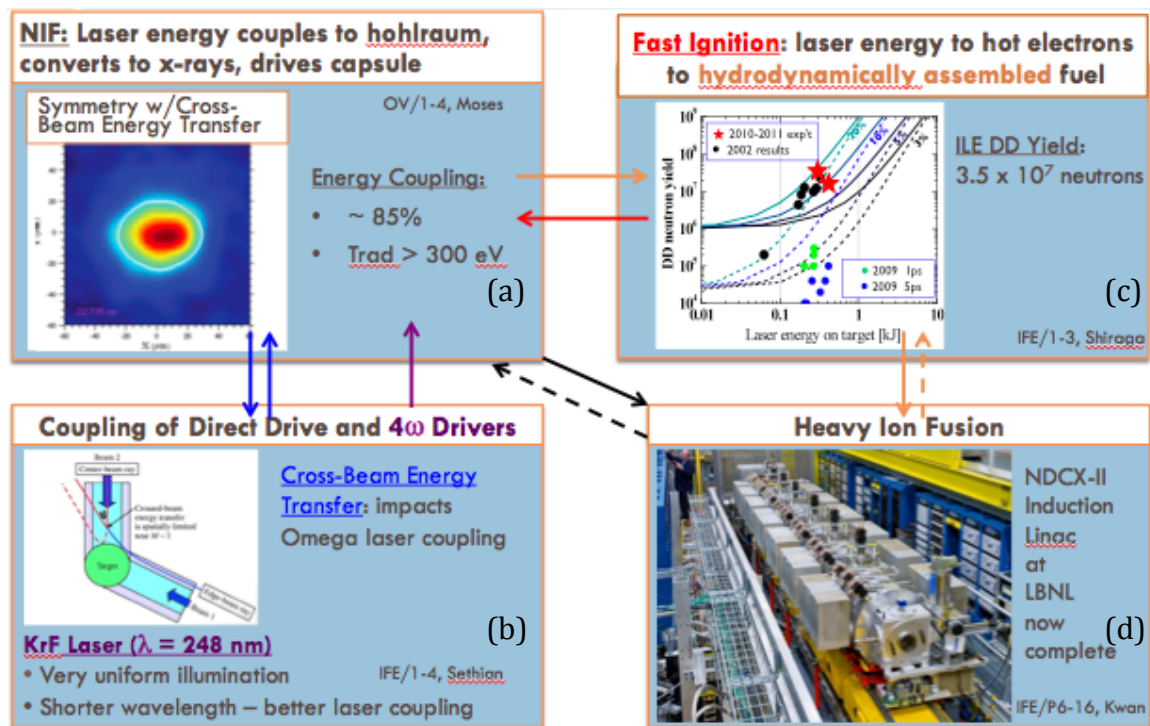
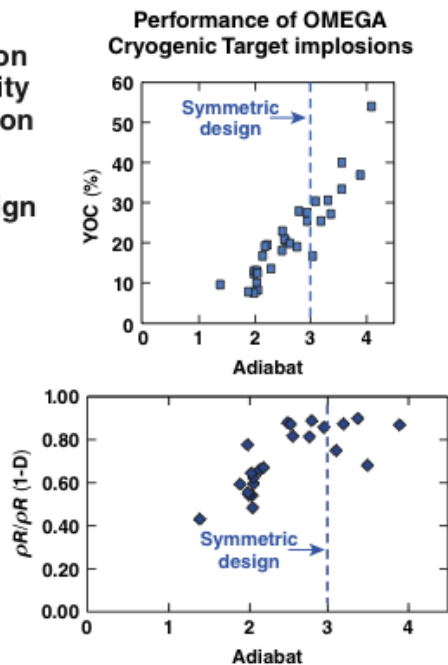


Fig. 3

Direct-drive ICF research has made significant progress since the 2010 IAEA meeting – R.L. McCrory IFE 1-2



- Polar drive will allow for direct-drive ignition experiments on the National Ignition Facility (NIF) with the x-ray-drive beam configuration
- OMEGA symmetric direct-drive cryogenic target implosions are defining the PD design space for the NIF
- Performance continues to improve:
 - neutron yields exceeding 10^{13} (up to ~40% of clean 1-D simulations)
 - ion temperature increased from 2.2 to 3 keV
 - $P\tau$ increased from 1.7 to 2.6 atm-s
- Initial polar-drive implosions have been performed on the NIF



TC10136

Fig. 4

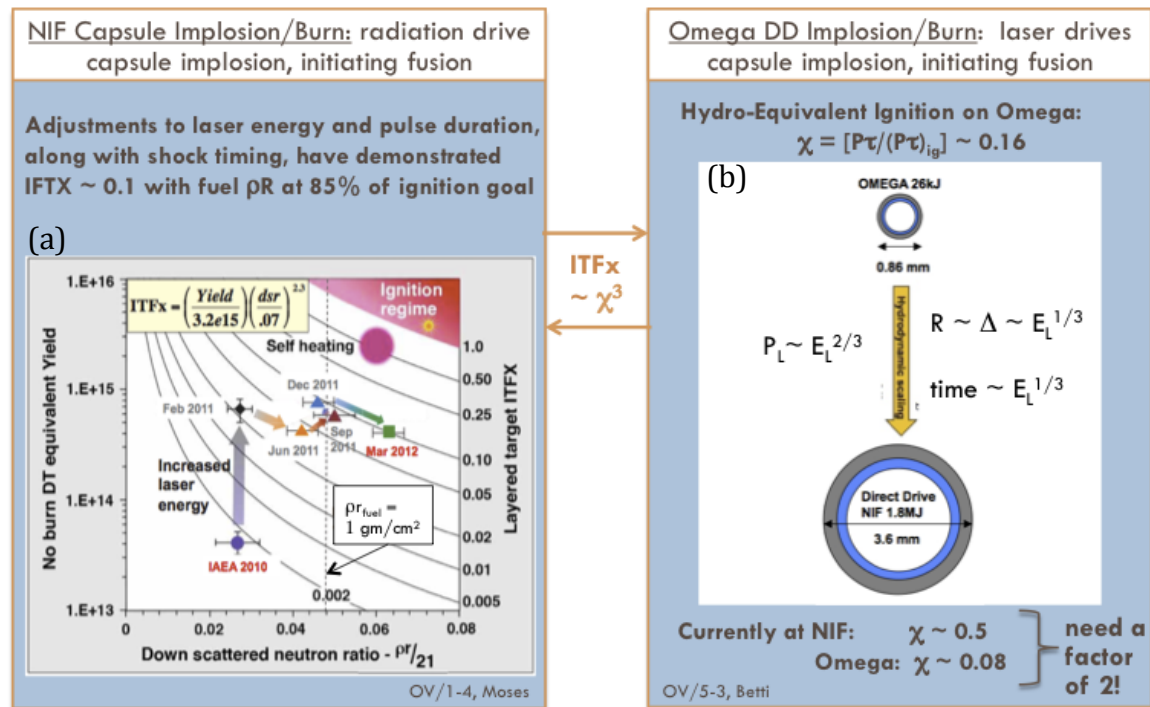


Fig. 5

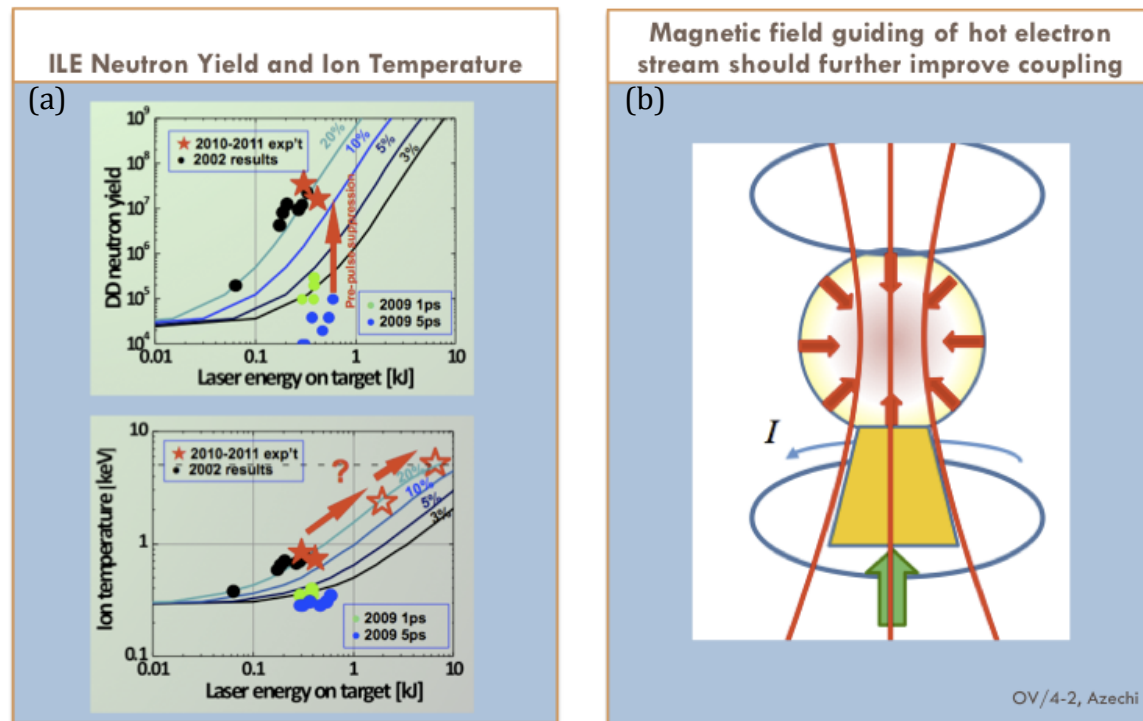


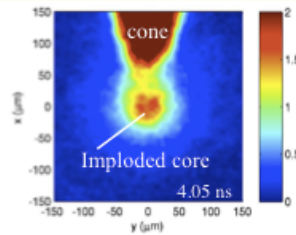
Fig. 6

The U.S. fast ignition (FI) team has made significant progress on detailed FI physics study with new platforms at the Omega laser facility

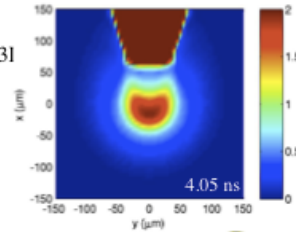
- Measured highest density ($\rho r \sim 0.3 \text{ g/cm}^2$) in FI cone-in-shell implosion, consistent with rad-hydro DRACO modeling results
- First-time imaging of energy flow into imploded cone-guided FI targets

8 keV Radiography for fuel assembly (led by LLE)

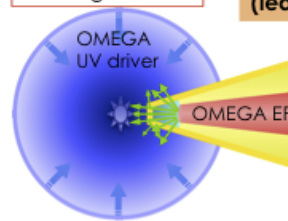
Experiment



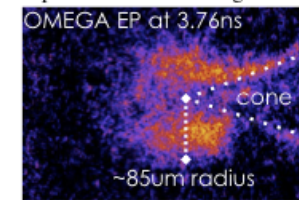
DRACO/Spec31 simulation



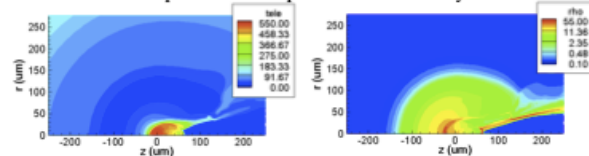
Cone guided FI



Imaging fast electron energy flow via fluorescence measurements (led by UCSD/GA)

Experiment: Cu K α image

DRACO predicted temperature and density at 3.76 ns



1. W. Theobald et al., Phys. Plasmas 18, 056305 (2011)
2. A.A. Solodov et al., AAC (2012)
3. F.N. Beg et al., SSAA symposium (2012)



Fig. 7

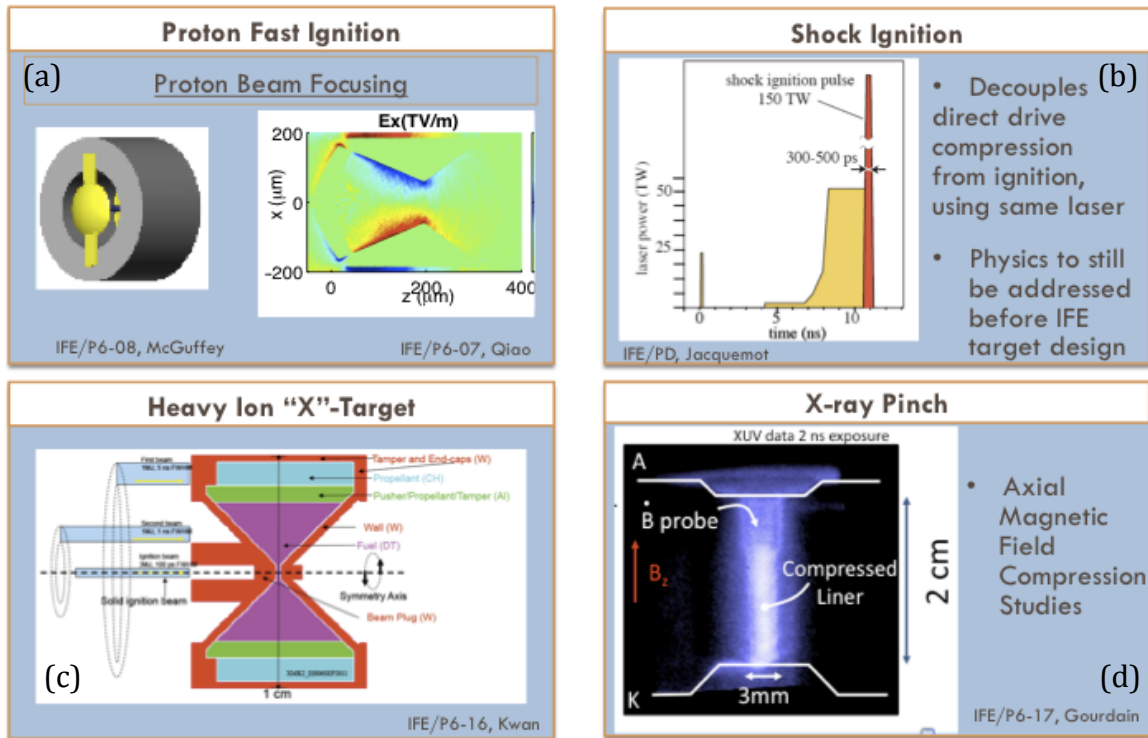


Fig. 8

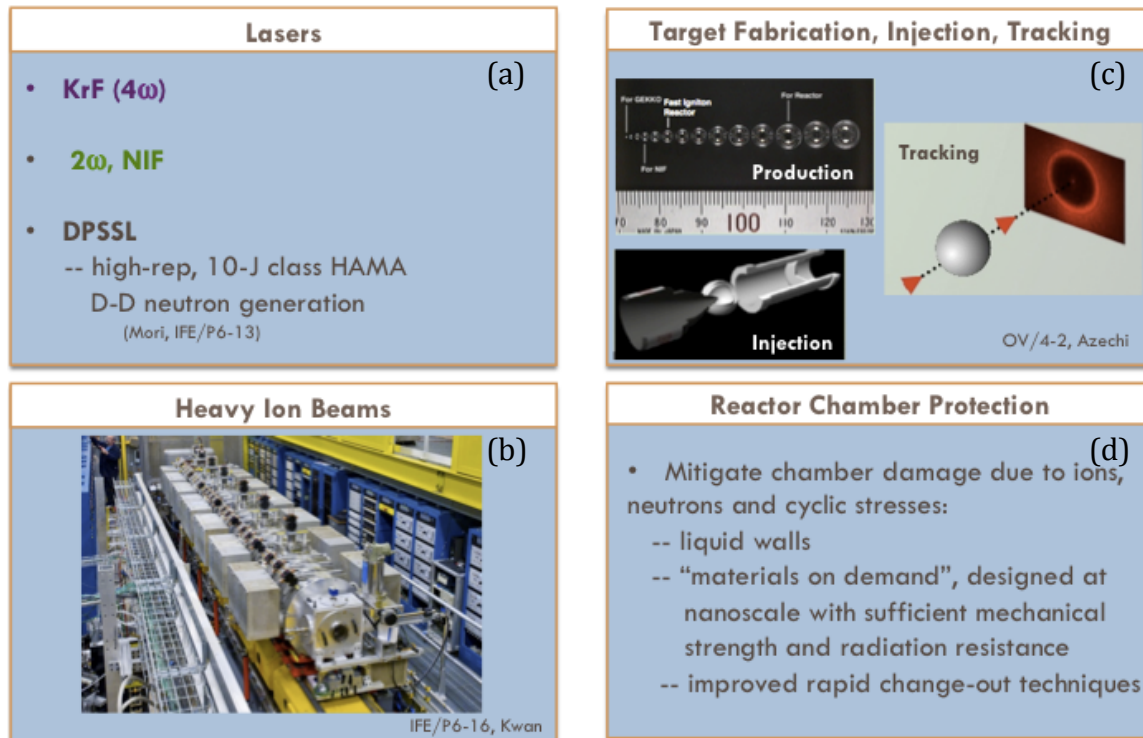
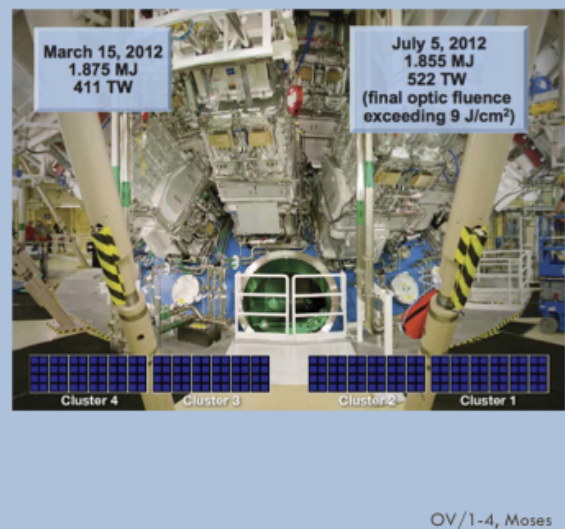


Fig. 9

NIF surpassed its milestone of delivering 1.8 MJ of 3 ω energy and 500 TW of power on target (a)



Precision at NIF enables exquisite tuning and reproducibility (b)

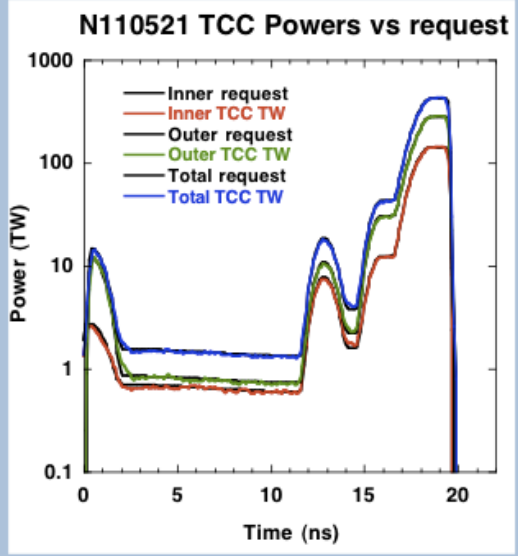


Fig. 10

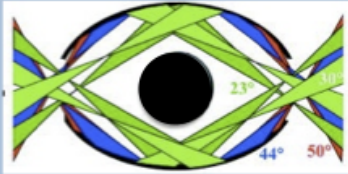
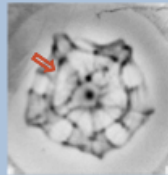
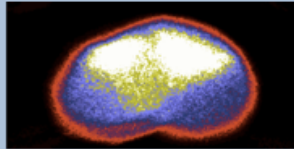
Improve Inner Beam Propagation (a)	Reduce SRS/hot electrons (b)	New diagnostics to research energy coupling (c)
<ul style="list-style-type: none"> • <i>Reduces amount of required cross-beam energy transfer</i> • Change geometry: -- <i>Rugby Hohlraum</i>: more headroom over capsule for same wall area  <ul style="list-style-type: none"> • Change hohlraum fill: -- <i>higher-Z fill</i> (gas, foam, ...) to increase T_e 	<ul style="list-style-type: none"> • Stimulated Raman Scatter (SRS): laser scatters off self-generated electron plasma waves; hot electron production • Stimulated Brillouin Scatter (SBS): laser scatters off self-generated ion acoustic waves • Hard x-ray images of capsule: no evidence of hot electron coupling • SBS-only target: -- <i>fill composition</i> • Increase T_e 	<ul style="list-style-type: none"> • Plasma characterization via Thomson scatter • Proton Deflectometry  IFE/P6-10, Li • Further characterization of crossed-beam energy transfer 

Fig. 11

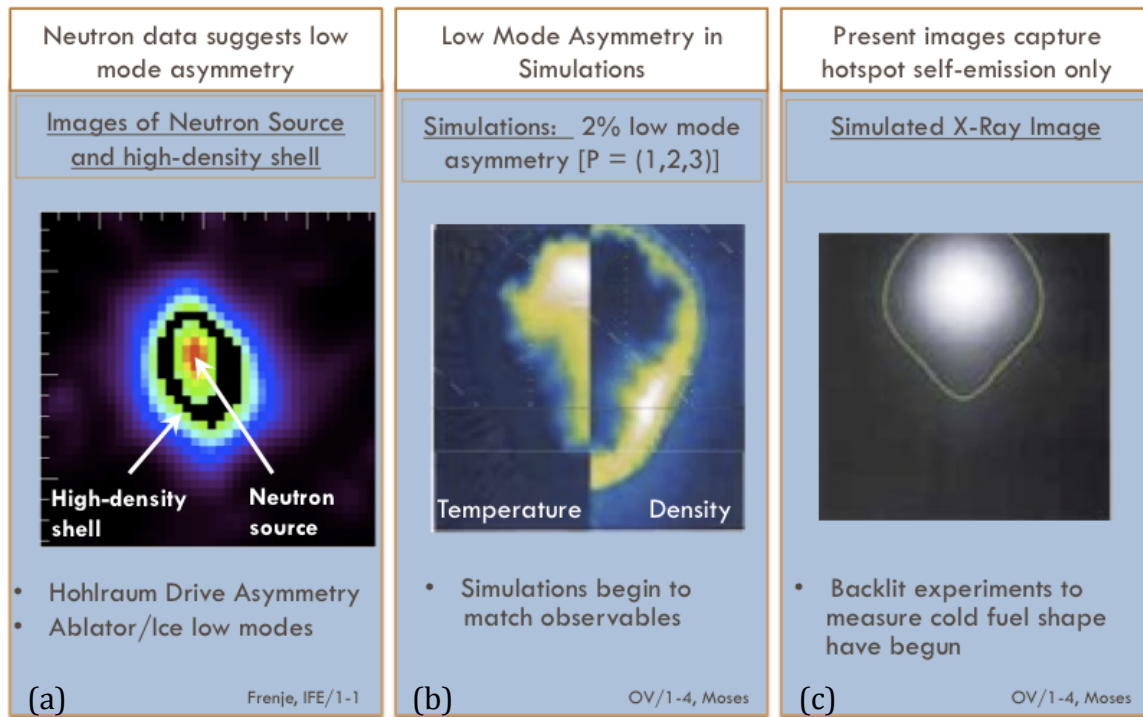


Fig. 12

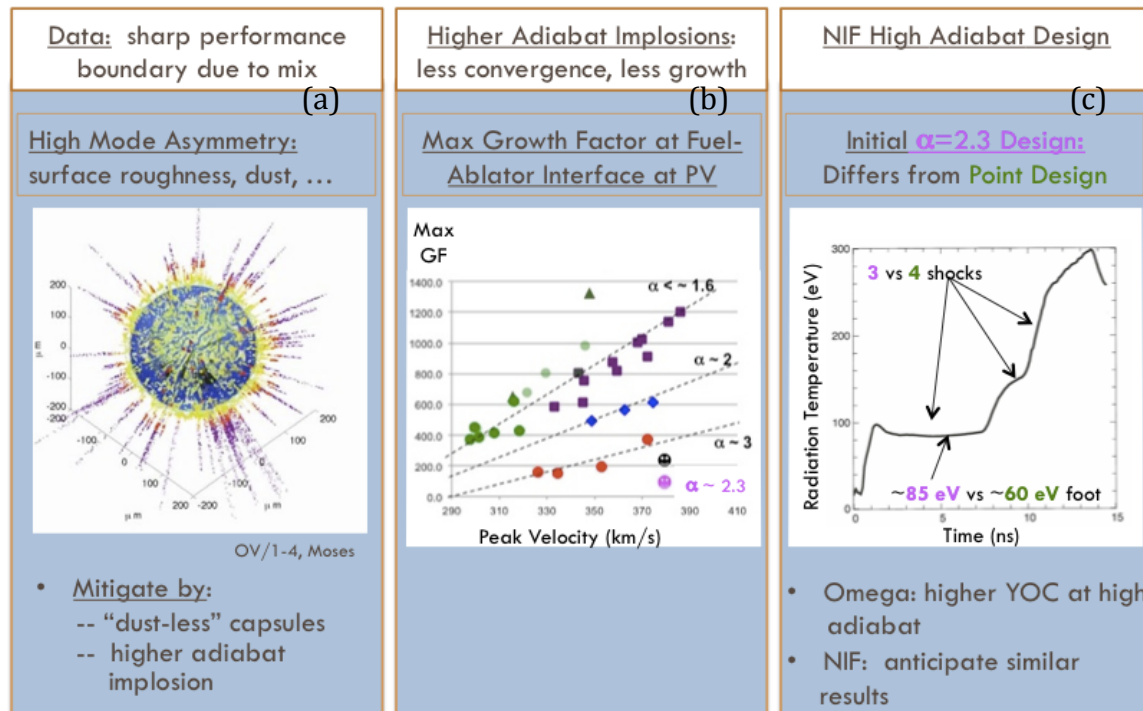


Fig. 13

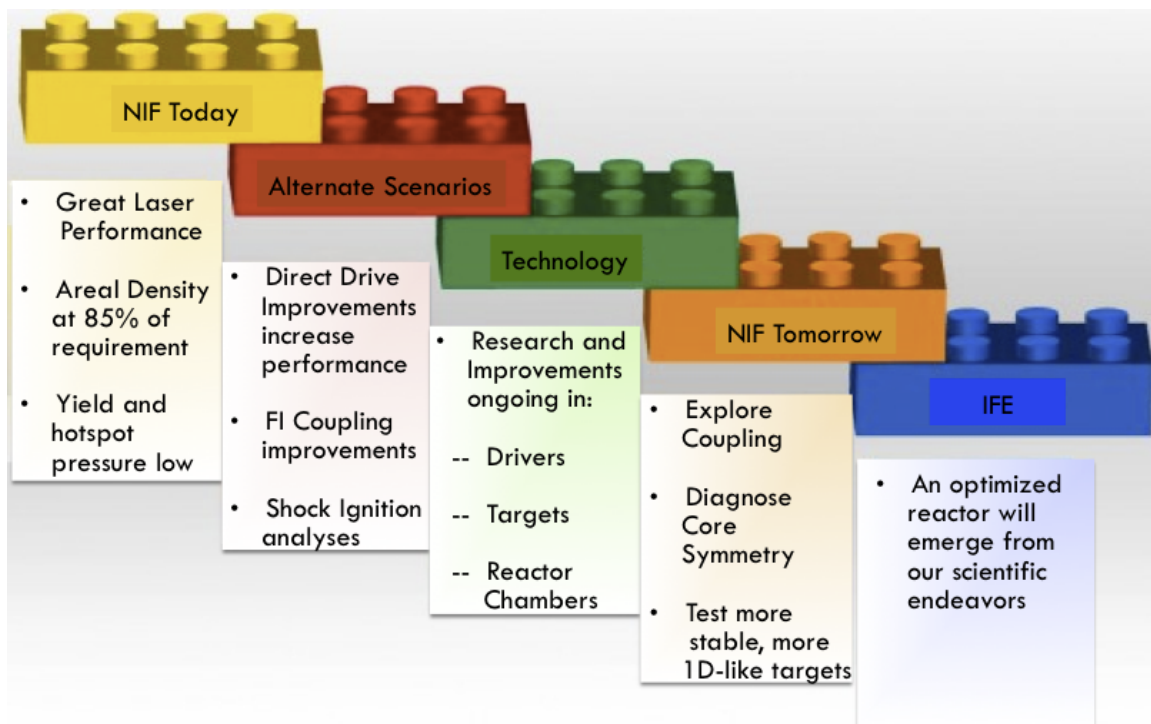


Fig. 14